Efficiency Considerations for the Purely Tapered Interference Fit (TIF) Abutments Used in Dental Implants

Dinçer Bozkaya
Graduate Student

Sinan Müftü*
Ph.D., Associate Professor

Northeastern University,
Department of Mechanical Engineering,
Boston, MA 02115

A tapered interference fit provides a mechanically reliable retention mechanism for the implant-abutment interface in a dental implant. Understanding the mechanical properties of the tapered interface with or without a screw at the bottom has been the subject of a considerable amount of studies involving experiments and finite element (FE) analysis. In this paper, approximate closed-form formulas are developed to analyze the mechanics of a tapered interference fit. In particular, the insertion force, the efficiency, defined as the ratio of the pull-out force to insertion force, and the critical insertion depth, which causes the onset of plastic deformation, are analyzed. It is shown that the insertion force is a function of the taper angle, the contact length, the inner and outer radii of the implant, the static and the kinetic coefficients of friction, and the elastic modulii of the implant/abutment materials. The efficiency of the tapered interference fit, which is defined as the ratio of the pull-out force to insertion force, is found to be greater than one, for taper angles that are less than 6 deg when the friction coefficient is 0.3. A safe range of insertion forces has been shown to exist. The lower end of this range depends on the maximum pull-out force that may occur due to occlusion in the multiple tooth restorations and the efficiency of the system; and the upper end of this range depends on the plastic deformation of the abutment and the implant due to interference fit. It has been shown that using a small taper angle and a long contact length widens the safe range of insertion forces. [DOI: 10.1115/1.1784473]

Introduction

A dental implant is a prosthetic device of alloplastic material implanted into the oral tissues beneath the mucosa and periosteal tissues and into the jaw bone to support a fixed or removable prosthesis. An abutment is the component of the dental implant system, which helps the soft tissue heal around it, or serves to support and/or retain the prosthesis. Prosthetic abutments can be connected to the implant immediately following surgical placement or after osseointegration takes place depending on the decision of timing of the loading. The abutment is retained in the implant by employing a mechanical attachment method. Ideally, the abutment should stay fixed with respect to the implant throughout the life of the implant. In the most common mechanical attachment method, the abutment is secured to the implant by using a retaining-screw. In other designs, a taper-integrated screw (TIS) or a purely tapered interference fit (TIF) are used in order to connect the implant and the abutment.

Reliability of the abutment retention mechanism is an important consideration for the implant biomechanics and clinical success, as the instability of the implant-abutment interface is one of the most commonly observed modes of implant complications [1]. In particular, in single tooth replacements screw loosening can be a problem. The mechanical design of the connection method, which is influenced by biological and clinical factors, has a significant effect on the reliability of the implant-abutment interface, and thus directly influences the long-term success of an implant system.

Occlusal forces on dental abutments act in different directions and magnitudes. The axial component of the occlusal force is predominantly compressive for a single tooth restoration. However, for multiple tooth restorations supporting a bridge, the axial component of the occlusal force could become tensile with a magnitude as large as 450 N [2]. Design of the implant-abutment interface should consider these loading mechanisms. In TIF type systems, tensile forces and loosening torques are the loading types that could result in abutment loosening. In systems that rely on screwed-in connections, compressive forces and loosening torques could do the same.

Approximately 80% of the implants sold in the United States feature a pure screw-type implant-abutment (IA) connection mechanism [3] which is represented by the design by Nobel Biocare (Nobel Biocare AB, Göteborg, Sweden) external hex implant body in Fig. 1(*a*). High rate (up to 40%) of clinical complications related to the screw, such as loosening and fracture had been encountered with the screw-retained abutment connection mechanism, particularly in single tooth replacements [4,5]. Inadequate screw preload, the misfit of the mating components and rotational characteristics of the screws were considered to be the reasons leading to screw loosening or fracture [5]. These problems have been alleviated, in part by material selection and surface treatment, in the recent versions of this type of attachment method [6].

Screw loosening has been less problematic with the taper-integrated screwed-in (TIS) abutments, where the tapered, top end of the screw makes an interference fit with the implant [7–9]. In the TIS abutments, the connection is secured by the frictional forces on the screw threads and on the tapered section. Depending on the design, the contact area and the contact forces on the tapered section of the abutment are considerably larger as compared to those of the screw threads. Therefore, most of the resistance to loosening torques occurs in the tapered section [10].

In the TIS designs by Ankylos (Degussa Dental, Hanau-Wolfgang, Germany) and ITI (Institut Straumann AG, Walden-

*Corresponding author: Northeastern University, Department of Mechanical Engineering, 334 SN Boston, MA 02115. Telephone: 617-373-4743; fax: 617-373-2921; e-mail: smuftu@coe.neu.edu.

Contributed by the Bioengineering Division for publication in the JOURNAL OF BIOMECHANICAL ENGINEERING. Manuscript received by the Bioengineering Division October 13, 2003; revision received January 23, 2004. Associate Editor: D. Fhyrie.

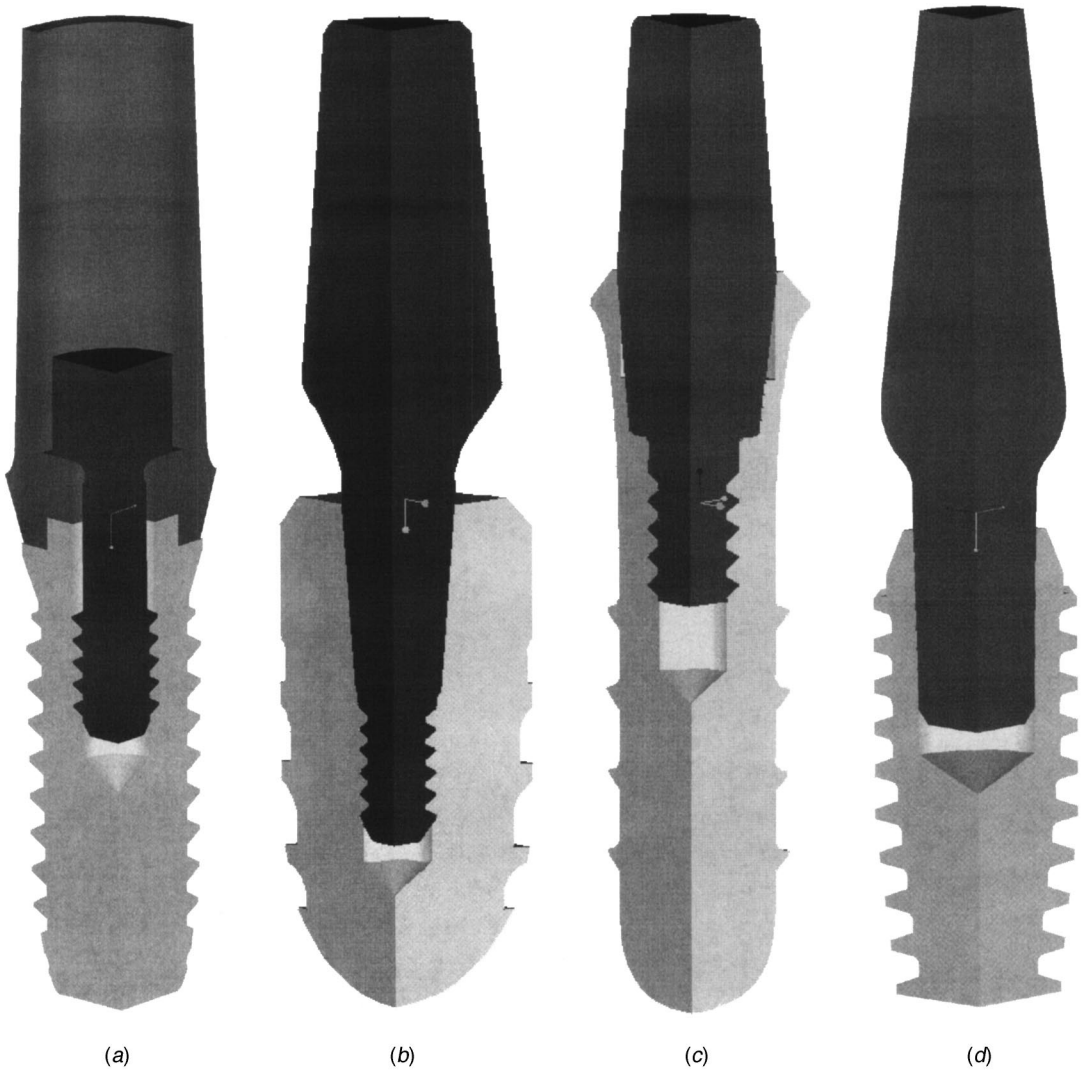

Fig. 1 Various implant-abutment attachment methods are used in commercially available dental implants. (*a*) screw only; (*b*) and (*c*) TIS; (*d*) TIF type attachment methods

burg, Switzerland), shown in Figs. 1(*b*) and 1(*c*), respectively, a tapered screw is incorporated to the end of the abutment, thus eliminating the need to use a third component. The market share of implant sales for the ITI system in the US is approximately 15% [3]. The prosthetic complication rate of 3.6% to 5.3%, for the ITI implant system is considerably lower than the retention mechanism using only a screw [7–9]. Mechanics of the TIS method for the ITI system is analyzed by finite element method by Merz et al. [7]. TIS type implants are investigated analytically in [10] where closed-form formulas are developed for estimating the tightening and loosening torque values.

The occlusal forces apply axial and tangential forces, and moments on the implants, in part due to the geometry of the prosthetic components [11]. This complicated loading mechanism could apply a large enough torque to loosen the abutment. Efficiency, defined as the ratio of the loosening torque to tightening torque, has been used as an evaluation metric for the TIS type IA connection method. Efficiency of the ITI system has been studied experimentally. At clinically relevant torque levels of 300–400 N-mm, different investigators found different efficiency ranges; 0.84–0.91 by Norton [12]; 1.1–1.15 Sutter et al. [13], and 0.79–1.06 Squire et al. [14]. The general range of efficiency was predicted to be 0.85–1.37, by Bozkaya and Müftü when the static coefficient μ_s was varied between 0.1 and 1 and the kinetic friction coefficient μ_k was varied between 70 and 100% of μ_s [10]. The authors showed that low efficiency was associated with low friction coefficient and high efficiency is related to the difference between the kinetic and static friction coefficients.

The third method of attachment uses a tapered abutment and an implant with a tapered receiving hole. The engagement of the abutment with the implant is provided by an impact force acting along the longitudinal axis of the abutment. The tapered interference fit (TIF) design by Bicon (Bicon Inc., Boston, MA, USA) is depicted in Fig. 1(*d*). The market share of TIF type implant systems is small compared to the implants using the other two connection methods mentioned above [2]. For this system, prosthetic complications related to IA connection mechanism failures were reported to be 0.74% for single tooth replacements [15]. Similar to the TIS type connection mechanism, the tapered surface of the TIF abutments create a relatively large frictional resistance area, and the interference fit provides the necessary large normal forces for frictional retention.

Previously, approximate analytical solutions for the contact pressure, the pull-out force and the loosening torque acting in a TIF-type system were developed, by modeling the tapered interference as a series of cylindrical interferences with variable radii by O'Callaghan et al. [16] and then by Bozkaya and Müftü [17].

These formulas were compared with nonlinear finite element analyses for different design parameters and the results agreed well [17]. An elastic-plastic finite element analysis of a TIF implant-abutment interface, with different insertion depths, showed that the stresses in the implant and abutment locally exceed the yield limit of the titanium alloy at the tips of the interface for an insertion depth of 0.10 mm. The plastic deformation region spreaded radially into the implant, for insertion depths greater than 0.1 mm. It was also found that the plastic deformation decreases the increase in the pull-out force due to increasing insertion depth. The optimum insertion depth was obtained when the implant starts to deform plastically [17].

A complete analytical solution of the tapered interference fit has not yet been reported. The cylindrical interference fit formulas, on the other hand, can be found in many textbooks including Shigley and Mischke [18]. The elastic-plastic analysis of cylindrical interference fits was studied, for example, by Gamer and Müftü [19].

This paper extends the discussion about the tapered interference fit given in a previous study by the authors [17]. In particular, approximate closed-form formulas are developed for a) estimating the *insertion* force; b) evaluating the efficiency of the TIF abutments; c) estimating the critical insertion depth, which causes the onset of plastic deformation; and, d) determining an insertion force range, which provides a safe pull-out force during occlusion and prevents plastic deformation in the material. These variables are investigated with respect to different parameters. The equations developed here, provide a relatively simple way of assessing the interdependence of the geometric and material properties of the system; and in one case, presented later, show a reasonably good match with experimental measurements of O'Callaghan et al. [16]. The important design variables that affect the retention and their effects are investigated.

Theory

Figure 2 describes the geometry of a TIF abutment system. The insertion force F_i required to seat a taper lock abutment into the matching implant is typically applied by tapping. The interference fit takes place, once the abutment is axially displaced by an amount Δz by tapping. Interference gives rise to contact pressure $p_c(z)$ whose magnitude changes along the axial direction z of the cone [17]. The resultant normal force N (Fig. 2(b)), acting normal to the tapered face of the abutment, is obtained by integrating $p_c(z)$ along the length s of the interference, [17]

$$N=\frac{\pi E\Delta z L_c \sin 2\theta}{6b_2^2}[3(b_2^2-r_{ab}^2)-L_c\sin\theta(3r_{ab}+L_c\sin\theta)] \tag{1}$$

where L_c is the contact length, b_2 is the outer radius of the implant, r_{ab} is the bottom radius of the abutment, θ is the taper angle as shown in Fig. 2, and, E is the elastic modulus of the implant and abutment, assumed to be made from the same material.

An average value for the insertion force F_i can be found from the energy balance, where the work done by the insertion force W_i is equal to the sum of the work done against friction W_f and the strain energy U_t stored in the abutment and the implant. This is expressed as,

$$W_i=F_i\Delta z=W_f+U_t. \tag{2}$$

The work done against friction W_f by sliding a tangential force $\mu_k N$ along the side s of the taper, by a distance Δs, is found from,

$$W_f=\mu_k\int_0^{\Delta s}N ds=\mu_k\int_0^{\Delta z}N\frac{dz}{\cos\theta} \tag{3}$$

where μ_k is the kinetic coefficient of friction, and the geometric relation $\Delta s=\Delta z/\cos\theta$ is used. Note that, in this equation the kinetic friction coefficient is used, as abutment insertion is a dynamic process. The work done against friction is calculated from Eqs. (1) and (3) as,

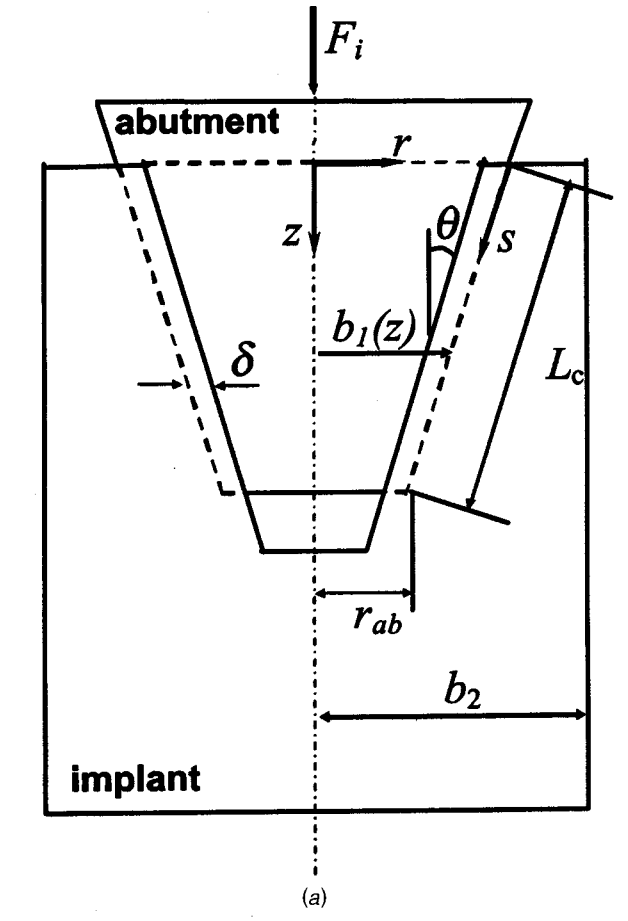

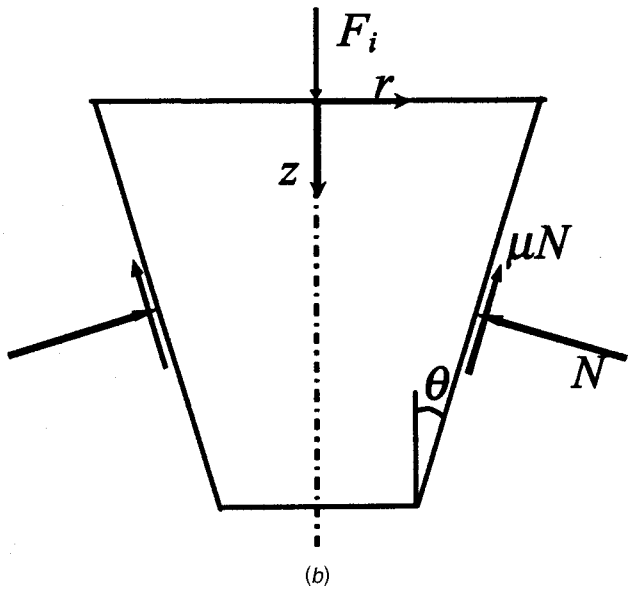

Fig. 2 (*a*) Definition of the design parameters of the tapered interface. (*b*) The free body diagram of the tapered abutment depicting the force balance during insertion.

$$W_f=\frac{\pi\mu_k E\Delta z^2 L_c\sin\theta}{6b_2^2}[3(b_2^2-r_{ab}^2)-L_c\sin\theta(3r_{ab}+L_c\sin\theta)]. \tag{4}$$

During the insertion of the abutment, some portion of the work

done by the insertion force is stored as strain energy in the abutment and the implant. The total strain energy U_t of the system is given by,

$$U_t = \int_0^{L_c \cos\theta} \int_0^{b_1} \pi r(\sigma_{rr}^a \varepsilon_{rr}^a + \sigma_{\theta\theta}^a \varepsilon_{\theta\theta}^a) dr dz + \int_0^{L_c \cos\theta} \int_{b_1}^{b_2} \pi r(\sigma_{rr}^i \varepsilon_{rr}^i + \sigma_{\theta\theta}^i \varepsilon_{\theta\theta}^i) dr dz, \quad (5)$$

where the radial and tangential stresses are σ_{rr} and $\sigma_{\theta\theta}$, and the radial and tangential strains are ε_{rr} and $\varepsilon_{\theta\theta}$, and the superscript a and i refer to the abutment and the implant, respectively. The radius of the abutment b_1 varies along the axial direction z as $b_1(z) = r_{ab} + (L_c \cos\theta - z)\tan\theta$. The stresses and strains for a TIF connection can be approximated as follows [17],

$$\sigma_{rr}^a = \sigma_{\theta\theta}^a = -\frac{E\Delta z \tan\theta}{2b_1(z)}\left[1 - \left(\frac{b_1(z)}{b_2}\right)^2\right] \quad (6)$$

$$\varepsilon_{rr}^a = \varepsilon_{\theta\theta}^a = -\frac{\Delta z \tan\theta(1-\nu)}{2b_1(z)}\left[1 - \left(\frac{b_1(z)}{b_2}\right)^2\right] \quad (7)$$

$$\sigma_{rr}^i = \frac{E\Delta z b_1(z)\tan\theta}{2b_2^2}\left[1 - \left(\frac{b_2}{r}\right)^2\right];$$

$$\sigma_{\theta\theta}^i = \frac{E\delta z b_1(z)\tan\theta}{2b_2^2}\left[1 + \left(\frac{b_2}{r}\right)^2\right] \quad (8)$$

$$\varepsilon_{rr}^i = \frac{b_1(z)\Delta z \tan}{2b_2^2}\left[-(1+\nu)\left(\frac{b_2}{r}\right)^2 + (1-\nu)\right];$$

$$\varepsilon_{\theta\theta}^i = \frac{b_1(z)\Delta z \tan\theta}{2b_2^2}\left[(1+\nu)\left(\frac{b_2}{r}\right)^2 + (1-\nu)\right] \quad (9)$$

where ν is the Poisson's ratio.

The total strain energy U_t of the system is calculated by using Eqs. (5)–(9). Once U_t is evaluated, the insertion force F_i can be found in closed form, from Eqs. (2) and (4). This expression is not given here in order to conserve space. However, its results are presented later in the paper.

Efficiency of a Tapered Interference Fit Abutment. The efficiency η of a TIF type abutment system is defined here as the ratio of the pull-out force F_p to the insertion force F_i,

$$\eta = \frac{F_p}{F_i}. \quad (10)$$

An approximate relation for the efficiency can be obtained by noting that in Eqs. (1)–(9) the strain energy U_t of the system is small as compared to the work done against friction. For example, the strain energy U_t of the system is approximately 6% of the total work done W_i for a 5 mm implant-abutment system, using the parameters given in Table 1. With this assumption the insertion force can be approximated by considering only the work done against friction ($W_i \cong W_f$) as,

$$\tilde{F}_i = \frac{\pi\mu_k E\Delta z L_c \sin\theta}{6b_2^2}[3(b_2^2 - r_{ab}^2) - L_c \sin\theta[3r_{ab} + L_c \sin\theta]]. \quad (11)$$

The pull-out force of the tapered interference was given by Bozkaya and Müftü as [17],

$$F_p = \frac{\pi E\Delta z L_c}{3b_2^2}[3(b_2^2 - r_{ab}^2) - L_c \sin\theta[3r_{ab} + L_c \sin\theta]](\mu_s \cos\theta - \sin\theta)\cos^2\theta \quad (12)$$

Table 1 The parameters of the tapered interface in three commercially available systems. Bicon (implant: 260-750-308; abutment: 260-750-301; ITI implant: 043.241S and the matching ITI-abutment: 048.542; and Ankylos part number 3101-00530). The parameters of Bicon were taken as the base and the ranges of variables were tested using the developed relations.

	Base Values			Range of Parameters Used for TIF System
	ITI	Ankylos	Bicon	
θ (°)	8	5.5	1.5	1–10
μ^*	0.3	0.3	0.3	0.1–1
μ_k/μ_s	1	1	1	0.7, 0.9, 1
L_c (mm)	0.73	3	3.25	0–5
b_2 (mm)	2.24	2.76	1.37	1–4
Δz (μm)	5	0.75	0.15	0–5
r_{ab} (mm)	1.42	0.97	0.76	–
E (GPa)	113.8	113.8	113.8	–
σ_Y (MPa)	–	–	950	–
R_c	–	–	1	–

*μ is the friction coefficient when it is assumed that $\mu_s = \mu_k$.

where the static coefficient of friction μ_s is used, as the pull-out force is applied on the initially stationary implant. The following simplified efficiency η' formula for the TIF type abutment is obtained by using Eqs. (11) and (12),

$$\eta' = \frac{F_p}{\tilde{F}_i} = \frac{2\cos\theta}{\mu_k}(\mu_s \cos\theta - \sin\theta). \quad (13)$$

The relative error ε involved in using Eq. (11) to find the insertion force is evaluated as,

$$\varepsilon = \frac{(W_f + U_t)/\Delta z - W_f/\Delta z}{(W_f + U_t)/\Delta z} = \frac{U_t}{W_f + U_t} = 1 - \frac{W_f}{W_f + U_t}. \quad (14)$$

Critical Insertion Depth. The interference fit results in a stress variation in the implant and the abutment as predicted by Eqs. (6)–(9). Typical circumferential $\sigma_{\theta\theta}$ and radial σ_{rr} stress variation along the radial direction (r/r_{ab}) in the abutment and the implant, as predicted by these formulas, is presented in Fig. 3, for different locations (z) along the contact length L_c. This figure shows that the maximum stresses occur in the implant, at location $z = L_c \cos\theta$, where the abutment radius is $b_1 = r_{ab}$. It is clear, from Eqs. (6)–(9), that both radial and circumferential stresses are

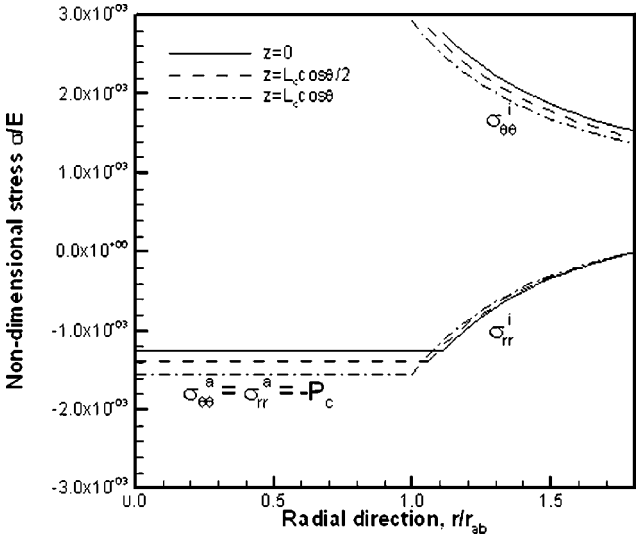

Fig. 3 The distribution of the radial and circumferential stresses in the abutment and the implant at different axial (z) locations

linearly proportional to the insertion depth Δz. Thus a critical insertion depth value exists, which causes plastic deformation of the implant material. The von Mises stress yield criterion is used to determine the onset of yielding. The equivalent von Mises stress is defined as,

$$\sigma = \frac{1}{\sqrt{2}}((\sigma_1-\sigma_2)^2+(\sigma_1-\sigma_3)^2+(\sigma_3-\sigma_2)^2)^{1/2} \qquad (15)$$

where the principal stresses σ_1, σ_2 and σ_3 are $\sigma_{\theta\theta}$, 0 and σ_{rr} respectively. Then by evaluating $\sigma_{\theta\theta}$ and σ_{rr} at $z = L_c \cos\theta$ and $b_1 = r_{ab}$ from Eqs. 8(*a*) and 8(*b*), the following relation for the critical insertion depth Δz_p, which causes the onset of plastic deformation can be obtained from Eq. (15),

$$\Delta z_p = R_c^{-1}\left(\frac{\sigma_Y}{E}\right)\frac{r_{ab}}{\tan\theta}\left[\left(\frac{r_{ab}}{b_2}\right)^2+\left(\frac{b_2}{r_{ab}}\right)^2\right]^{-1/2} \qquad (16)$$

where σ_Y is the yield strength of the implant material obtained from uniaxial tension test, and R_c is a stress concentration factor. It should be noted that the plain stress elasticity approach used here provides only approximate answers. One drawback, of this approach is that it does not capture the stress concentrations at the ends of the contact region [17]. The stress concentration factor R_c, which should have a value greater than one, could be used to take this effect into account.

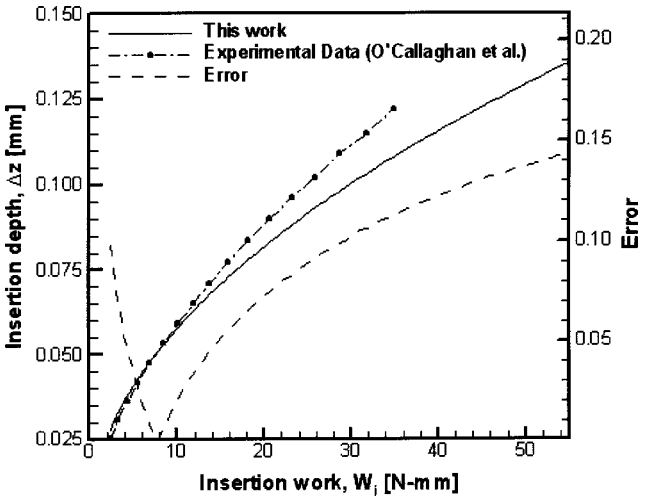

Fig. 4 The insertion depth as a function of work of insertion. Experimental results of O'Callaghan et al. [16] represented by the curve fit formula, $\Delta z = 1.55\times10^{-2} W_i^{0.579}$ are compared with the results of this work calculated for the base parameters of Bicon system.

Results

The design formulas developed above are used to evaluate the effects of various design parameters on the connection stability of a TIF system. The design parameters are applied in a relatively wide range around the base values, taken from a Bicon implant, which is the most widely used TIF type implant system, albeit with a small share of the U.S. market [2]. The geometric and material properties of this system are given in Table 1, along with the properties of the tapered section of the ITI and Ankylos systems. This table shows that the geometric parameters are similar between these systems, with the exception of the taper angle where the TIF system has the smallest taper angle. The geometric parameters of the TIF system are varied in the neighborhood of its base parameters. In selecting the applied ranges, indicated in Table 1, practical implant size and values of the Ankylos and ITI systems were considered.

Checking the Insertion Depth Formula. In Fig. 4, the insertion depth Δz is plotted as a function of work done during insertion W_i $(=F_i \Delta z)$. The solid lines indicate the predictions based on the formulas developed here, and the circles indicate the curve fit to the experimental results of O'Callaghan et al. [16]. The curve fit, which is valid in the range $0.025 \leq \Delta z \leq 0.15$ mm, is given by O'Callaghan et al. as $\Delta z = 1.55\times10^{-2} W_i^{0.579}$, where the units of Δz and W_i are mm and N-mm, respectively (Fig. 4). On the other hand, by considering, for example, the simplified insertion force formula $\tilde{F}_i$ given in Eq. (11), the insertion depth Δz is found to be proportional to $W_i^{0.5}$. The error between the experimental curve fit formula and this work is plotted as broken lines in Fig. 4, and is seen to be less than 20%. The discrepancy is largely due to the plastic deformation of the implant, which is predicted to start around $\Delta z = 0.13$ mm and occupy a wider area at deeper Δz values. Therefore, it is concluded that Eq. (11) provides a fairly good estimate of the insertion force F_i, when the material remains elastic.

Critical Insertion Depth. Figure 5(*a*) shows the effect of the bottom radius of the abutment r_{ab} on the critical insertion depth Δz_p (Eq. (16)) for different taper angles θ. This figure demonstrates that if a design has small radius r_{ab} and a large taper angle θ, then onset of plastic deformation occurs at a lower insertion-depth value Δz. Figure 5(*b*) shows the variation of the critical insertion depth Δz_p with the outer radius b_2 of the implant for different abutment radii r_{ab}. This figure indicates that the critical insertion depth decreases with increasing implant outer radius. This result may seem counter intuitive at first, but it can be explained by noting that the contact pressure also increases with b_2 at the tip of the abutment [17]. Therefore, the stress levels rise with increasing $(b_2 - r_{ab})$ distance. On the other hand, for a fixed value of implant radius b_2, increasing the abutment radius r_{ab} has the effect of increasing the value of the critical insertion depth.

Effects of System Parameters on Efficiency. The effect of the design parameters on the efficiency η of the system is investigated for the TIF interface in Fig. 6, using Eqs. (10) and (13) with complete (F_i) and simplified $(\tilde{F}_i)$ insertion force formulas. Investigation of Eq. (13) shows that the efficiency of the interface η' depends on the kinetic and static coefficients of friction μ, and taper angle θ. In Fig. 6, both the complete η and simplified η' efficiency relations are plotted for different taper angles θ in the range 1–10 deg, coefficient of friction μ $(=\mu_k=\mu_s)$ in the range 0.1–0.9 and the kinetic coefficient of friction as a fraction of static coefficient of friction μ_k/μ_s in the range 0.7–1 for $\mu_s = 0.5$. Figure 6(*a*) and Fig. 6(*c*) show that increasing θ and μ_k/μ_s results in efficiency reduction, whereas Figure 6(*b*) shows that increasing μ $(=\mu_k=\mu_s)$ results in efficiency increase. For θ smaller than 5.8 deg, one finds $\eta > 1$. For large taper angles, such as $\theta = 10$ deg, the efficiency of the interface is around 0.5. Increasing coefficient of friction from 0.1 to 0.2 increases the efficiency from 1.24 to 1.56. A further increase in the coefficient of friction results in an increase in the efficiency with decreasing slope as shown in Figure 6(*b*). As the difference between static and kinetic coefficient of friction is increased by taking the static friction coefficient larger, the efficiency of the system increases. A difference of 30% of the static friction coefficient results in an efficiency of 2.6.

The relative error ε between using F_i and $\tilde{F}_i$ is defined by Eq. (14). The accuracy of the simplified insertion force $\tilde{F}_i$ formula (Eq. (11)), which gives an insight to interdependence of the design parameters, is also investigated in Fig. 6. In general, it is seen that Eq. (13) overestimates the efficiency of the attachment. The relative error introduced by using $\tilde{F}_i$ increases with increasing θ and decreasing μ. The simplified formula can be used with less than 10% relative error for the following ranges, $0.2 \leq \mu \leq 0.9$ and 1 deg $\leq \theta \leq 2.4$ deg.

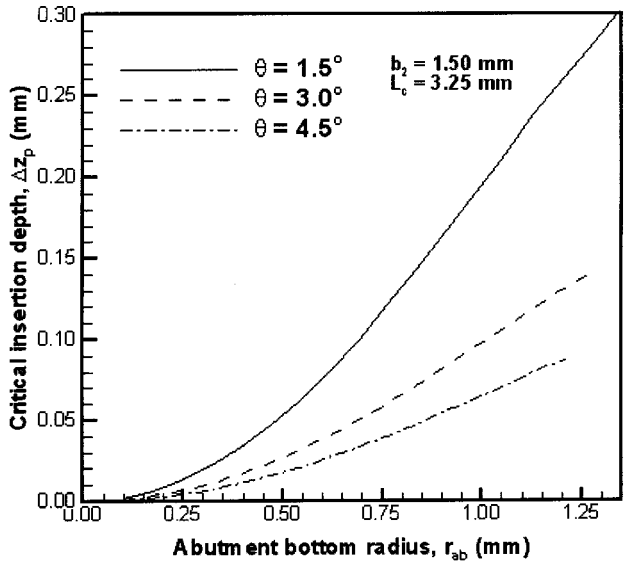

(*a*)

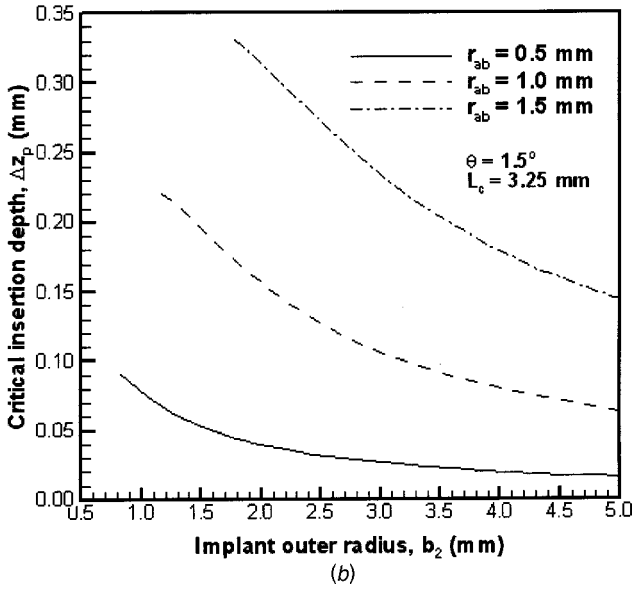

(*b*)

Fig. 5 The critical insertion depth Δz_p, which causes onset of plastic deformation as a function of (*a*) bottom radius of the abutment r_{ab} for different taper angles θ, and (*b*) implant outer radius b_2 for different r_{ab} values. The other parameters, which are fixed, are reported in Table 1.

Effects of System Parameters on Forces. In this work, the implant is assumed to be a cylinder. Commercially available implants are not cylindrical; they typically have a variable outer radius profile. This issue has been addressed in the authors' previous work, where it was shown that this condition introduces a small effect [17]. Eqs. (11) and (12) provide a relatively simple way of assessing the interdependence of the geometric and material properties of the system. For example, the magnitudes of the insertion $\tilde{F}_i$ and the pull-out F_p forces, found in Eqs. (11) and (12), depend on the parameters Δz, E, μ linearly; on the parameters b_2, r_{ab} parabolically; on the parameter L_c in a cubic manner; and, on the parameter θ trigonometrically. The details of these functional dependence are investigated next.

Effect of Taper Angle. Figure 7(*a*) shows the effect of taper angle θ on the insertion F_i and pull-out forces F_p. In evaluating this figure, the interference $\delta = \Delta z \tan\theta$ was kept constant at 4 μm

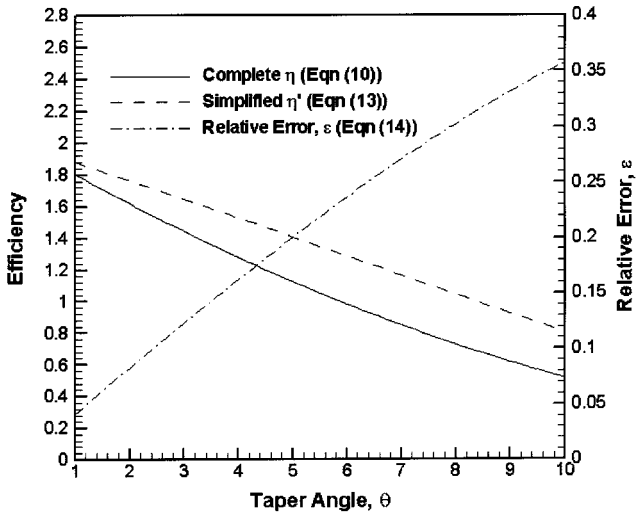

(*a*)

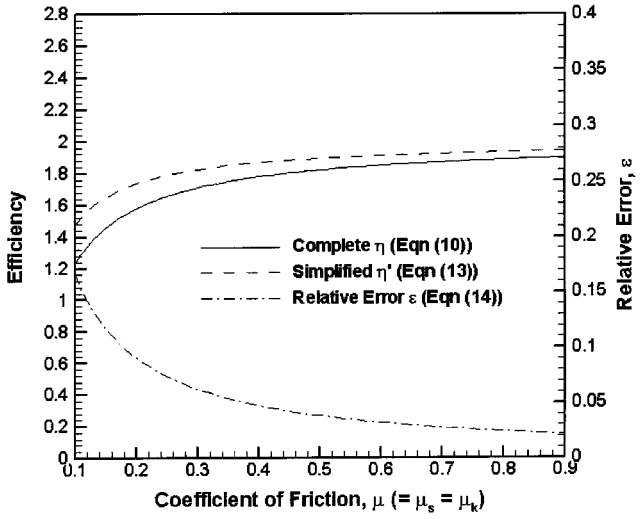

(*b*)

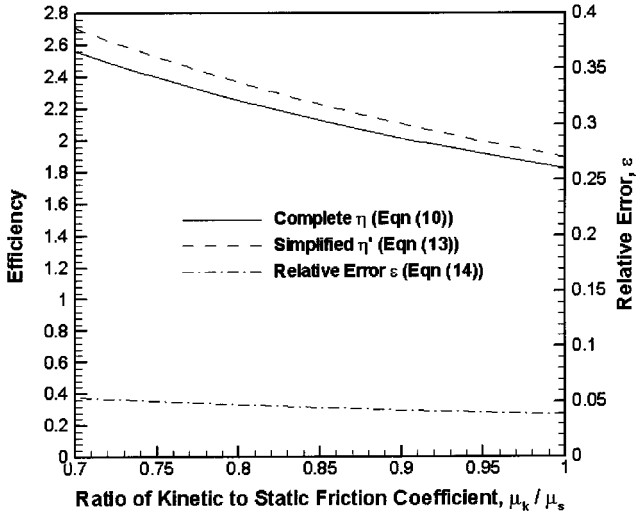

(*c*)

Fig. 6 The variation of the efficiency of the attachment with respect to different parameters. θ, μ and μ_k/μ_s are the significant parameters affecting the efficiency of the attachment. The other parameters, which are fixed, are reported in Table 1.

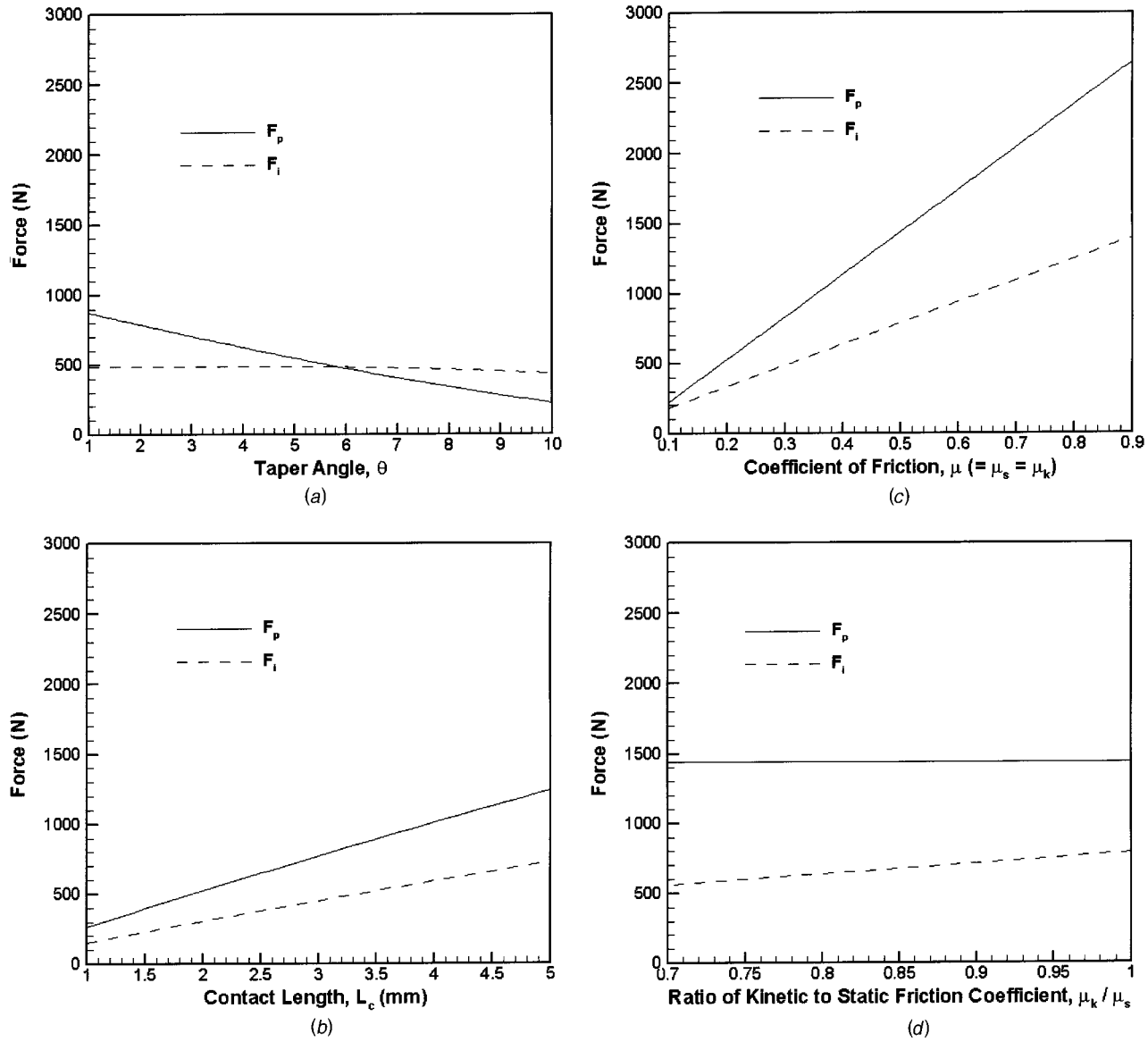

Fig. 7 Variation of pull-out F_p and insertion F_i force with (*a*) taper angle θ, (*b*) contact length L_c, (*c*) coefficient of friction, and (*d*) ratio of kinetic to static friction coefficient. The other parameters, which are held fixed, are reported in Table 1.

for $\theta = 1.5$ deg and $\Delta z = 0.1524$ mm. Keeping the δ value constant implies that the insertion force is kept approximately constant as the taper angle varies in the range 1–10 deg. In fact Figure 7(*a*) shows this assertion to be correct for the most part. The magnitude of the pull-out force F_p, on the other hand, decreases from 1750 N to 500 N in the same range. The pull-out force becomes less than the insertion force for taper angles greater than 5.8 deg. This figure in general shows that larger taper angles reduce the pull-out force; this is a situation, which should be avoided for the long term stability of the interface.

Effect of the Contact Length. The pull-out and insertion forces increase with the cube of the contact length L_c as shown in Eqs. (2) and (12). However, in the region of interest for dental implants, $1 < L_c \leq 5$ mm, this dependence appears linear, as shown in Figure 7(*b*). Increasing the contact length causes insertion force F_i to increase from 150 N at $L_c = 1$ mm to 700 N at $L_c = 5$ mm; In the same L_c range the pull-out force F_p varies between 290 N and 1250 N.

Effect of Friction. The coefficient of friction, despite its significant effects on the insertion and pull-out processes, is difficult to determine exactly. First, a distinction must be made between the static and kinetic coefficient of friction values; typically, the static coefficient of friction μ_s is greater than the kinetic coefficient of friction μ_k [20]. Second, the value of the coefficient of friction could be affected by the presence of saliva, which acts as a lubricant in the contact interface. The friction coefficient could also depend on the surface roughness and treatment [21]. With many factors affecting its value, it is important to understand the effect of a relatively wide range of friction coefficients, on the mechanics of the connection.

The dependence of the insertion force F_i on the kinetic friction coefficient μ_k, and the pull-out force F_p on the static friction coefficient μ_s are shown to be linear in Eqs. (2) and (12). Figure 7(*c*) demonstrates the effect of coefficient of friction when $\mu_k = \mu_s$. This figure shows that the pull-out force F_p is more adversely affected by the reduction of coefficient of friction. For example, at $\mu = 0.1$ the pull-out force is equal to the insertion force (200 N), but at $\mu = 0.7$ the pull-out force (2000 N) is nearly twice as much as the insertion force (1000 N). This behavior is also evident in the simplified efficiency formula, given in Eq.

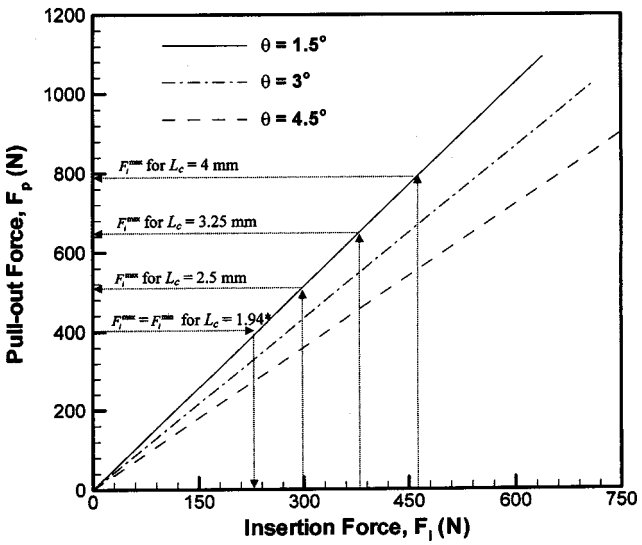

Fig. 8 The pull-out force F_p as a function of insertion force F_i, for different contact lengths L_c and taper angles θ.

(13), and plotted in Fig. 6(*b*). Close inspection of this formula shows that when $\mu_k = \mu_s$, and for infinite friction ($\mu \to \infty$) the simplified efficiency of the system behaves as $\eta' \to 2\cos^2\theta$. The complete and simplified efficiency formulas approach this limit in Fig. 6(*b*), which has the value of 1.997 for $\theta = 1.5$ deg. Figure 7(*d*) shows the effect of the kinetic coefficient of friction on the insertion force F_i by varying the ratio μ_k/μ_s in the range 0.7–1 for $\mu_s = 0.5$. This figure shows that the insertion force varies linearly in this range from 580 N to 800 N.

Range of Insertion Forces. Two factors limit the magnitude of the insertion force F_i to be applied to the abutment. First, F_i should be sufficiently large to seat the abutment securely, and hence provide enough frictional resistance to pull-out forces. Second, excessive plastic deformation of the implant and the abutment due to interference-fit should be avoided. The minimum admissible insertion force $F_i^{\min}$ should be based on the maximum pull-out force F_p which could occur during occlusion. Brunski states this value to be 450 N [2]. Then, for a given design, the $F_i^{\min}$ value can be found from Eq. (10). The maximum admissible insertion force $F_i^{\max}$ depends on the critical insertion depth Δz_p given by Eq. (16) and it is found as described in Eq. (2).

Next, the effects of the taper angle θ and the contact length L_c on the insertion force F_i are investigated. Arguably, θ and L_c are two of the many design parameters which could be changed without much impact on the biomechanics of the system. A relation between the insertion force and the pull-out force can be obtained from Eqs. (2) and (12); as both the insertion force F_i and the pull-out force F_p depend on insertion depth Δz in a linear fashion, their interdependence is also linear. Note that this linear dependence was also shown in an experimental work presented in reference [22].

The variation of the pull-out force F_p with respect to the insertion force F_i is plotted in Figure 8 for $\theta = 1.5$, 3, and 4.5 deg. The pull-out force is taken as 400 N. The maximum insertion force $F_i^{\max}$ is evaluated for different contact lengths of $L_c = 2.5$, 3.25, and 4 mm for $\theta = 1.5$ deg, as described above, and marked on the figure. This figure shows that as the contact length L_c decreases, the maximum admissible insertion force $F_i^{\max}$ also decreases. In fact, there exists a critical contact length where $F_i^{\min} = F_i^{\max}$. It is, therefore, concluded that, in order to allow a wide range of insertion force F_i for the clinician, a relatively long contact length L_c is necessary. The admissible range of insertion forces F_i for taper angle values of $\theta = 1.5$, 3 and 4 deg and contact length values of $L_c = 2.5$, 3.25 and 4 mm are presented in Table 2. This table shows that using a large taper angle θ has an adverse effect on the design; as the taper angle increases from 1.5 to 4.5 deg it is seen that the minimum insertion force increases, the admissible insertion force range narrows and the maximum pull-out force becomes lower.

Table 2 Minimum $F_i^{\min}$ and maximum $F_i^{\max}$ insertion forces and the corresponding pull-out forces F_p are listed for different taper angles θ and contact lengths L_c. "*" denotes the critical contact length when the minimum required insertion force is equal to the maximum insertion force.

θ [°]	L_c [mm]	η	$F_i^{\min}$–$F_i^{\max}$ [N]	$F_p^{\min}$–$F_p^{\max}$ [N]
1.5	1.94*	1.71	233–233	400–400
	2.50	1.71	233–298	400–510
	3.25	1.71	233–383	400–655
	4.00	1.71	233–465	400–795
3.0	2.25*	1.45	275–275	400–400
	2.50	1.45	275–304	400–439
	3.25	1.45	275–385	400–555
	4.00	1.45	275–461	400–663
4.5	2.72*	1.2	333–333	400–400
	3.25	1.2	333–385	400–462
	4.00	1.2	333–453	400–540

Summary and Conclusions

There may be significant differences in load magnitudes and directions acting on the abutment of a single tooth restoration, as compared to that of a multiple tooth restoration. In a single tooth restoration, the abutment could be subjected to a compressive axial load, a loosening torque and a bending moment. Therefore, pull-out is not expected to be a problem for a TIF type system. However, it has been shown that tensile axial forces may act on the abutments supporting multiple tooth restorations. This, along with the loosening torque, is the main load component that could cause abutment loosening in the TIF implants. The effects of loosening torques have been investigated in [17]. In this paper, the pull-out force is considered, along with insertion force, insertion efficiency and plastic deformation of the materials.

The tensile (pull-out, F_p) force value at which a TIF type abutment becomes loose is an indication of the stability of the implant-abutment connection. The present study showed that F_p is linearly proportional to the insertion force F_i and to the insertion depth Δz. The insertion force, which is provided by an impact, could be difficult to control and could vary between clinicians. A safe range of insertion forces has been shown to exist. The lower end $F_i^{\min}$ of this range is determined by the maximum pull-out force applied by occlusion and the efficiency of the system. The upper end $F_i^{\max}$ of this range is determined by the plastic deformation of the abutment and the implant due to interference fit. The effects of taper angle θ and contact length L_c on $F_i^{\min}$ and $F_i^{\max}$ have been investigated. It has been shown that small taper angle and long contact length improves the safe range of insertion forces.

It should be noted that in determining the safe-range of insertion forces, the other system parameters such as r_{ab}, b_2, E, μ_k, and μ_s could also be varied. However, often, there are practical constraints on these parameters. For example, E is constrained by the elastic modulus of the implant material, b_2 is constrained by the available bone space and the stresses transferred to the bone, and r_{ab} is constrained by b_2 and θ. Precise control of both of the friction coefficient values μ_s and μ_k is nearly impossible. Therefore, emphasis has been placed on varying the taper angle θ and the contact length L_c.

The efficiency η, which is defined as the ratio of the pull-out force to the insertion force is another significant parameter in evaluating the stability of the attachment. The taper angle θ and

friction coefficient are determined to be the parameters that have the most significant influences on the efficiency. Surprisingly, contact length L_c, implant radius b_2 and elastic modulus E have no significant effect on η. A large friction coefficient improves the efficiency of the interface. However, the friction coefficient could be subject to large uncertainties, due to various factors such as presence of saliva, surface finish of the mating components, etc. Therefore, use of a small taper angle in the designs ensures relatively high efficiency of the TIF type connection mechanism.

This study provides an insight into the effect of various parameters on the stability of the TIF type attachment method used in dental implants. Approximate closed form formulas are presented to evaluate the efficiency of the implant-abutment interface, as well as to suggest safe ranges of insertion forces. Future studies should include experimental determination of friction coefficients in dental implants under various loading and biological conditions.

Acknowledgments

The authors gratefully acknowledge the discussions they had with Mr. Fred Weekley (United Titanium, Wooster, OH) and the partial support of Bicon Implants (Bicon Inc., Boston, MA) for this work. The help of Dr. Ali Müftü (Tufts University, Boston, MA) during all stages of this work is also gratefully acknowledged.

References

[1] Scacchi, M., Merz, B. R., and Schär, A. R., 2000, ''The development of the ITI Dental Implant System,'' Clin. Oral Implants Res., **11**, pp. 22–32.
[2] Brunski, J. B., 1999, ''In vivo bone response to biomechanical loading at the bone/dental-implant interface,'' Adv. Dent. Res., **13**, pp. 99–119.
[3] Anonymous, 2001, ''U.S. Markets for Dental Implants 2001: Executive Summary,'' Implant Dent., **10**(4), pp. 234–237.
[4] Geng, J., Tan, K., and Liu, G., 2001, ''Application of finite element analysis in implant dentistry: A review of the literature,'' J. Prosthet. Dent., **85**, pp. 585–598.
[5] Schwarz, M. S., 2000, ''Mechanical complications of dental implants,'' Clin. Oral Implants Res., **11**, pp. 156–158.
[6] Martin, W. C., Woody, R. D., Miller, B. H., and Miller, A. W., 2001, ''Implant abutment screw rotations and preloads for four different screw materials and surfaces,'' J. Prosthet. Dent., **86**, pp. 24–32.
[7] Merz, B. R., Hunenbart, S., and Belser, U. C., 2000, ''Mechanics of the implant-abutment connection: An 8-degree taper compared to a butt joint connection,'' Int. J. Oral Maxillofac Implants, **15**, pp. 519–526.
[8] Levine, R. A., Clem, D. S., Wilson, Jr., T. G., Higginbottom, F., and Solnit, G., 1997, ''Multicenter retrospective analysis of the ITI implant system used for single-tooth replacements: Preliminary results at 6 or more months of loading,'' Int. J. Oral Maxillofac Implants, **12**, pp. 237–242.
[9] Levine, R. A., Clem, D. S., Wilson, Jr., T. G., Higginbottom, F., and Saunders, S. L., 1999, ''A multicenter retrospective analysis of the ITI implant system used for single-tooth replacements: Results of loading for 2 or more years,'' Int. J. Oral Maxillofac Implants, **14**, pp. 516–520.
[10] Bozkaya, D., and Müftü, S., 2004, ''Mechanics of the Taper Integrated Screwed-In (TIS) Abutments Used Dental Implants,'' accepted for publication J. Biomech.
[11] Warren Bidez, M. and Misch, C. E., 1999, ''Clinical biomechanics in implant dentistry,'' in Implant Dentistry, second edition, ed. Misch C. E., Mosby, St. Louis, MO, pp. 303–316.
[12] Norton, M. R., 1999, ''Assessment of cold welding of the internal conical interface of two commercially available implant systems,'' J. Prosthet. Dent., **81**, pp. 159–166.
[13] Sutter, F., Weber, H. P., Sorensen, J., and Belser, U., 1993, ''The new restorative concept of the ITI Dental Implant System: Design and engineering,'' Int. J. Periodontics Restorative Dent., **13**, pp. 409–431.
[14] Squier, R. S., Psoter, W. J., and Taylor, T. D., 2002, ''Removal torques of conical, tapered implant abutments: The effects of anodization and reduction of surface area,'' Int. J. Oral Maxillofac Implants, **17**, pp. 24–27.
[15] Müftü, A., and Chapman, R. J., 1998, ''Replacing posterior teeth with free-standing implants: four year prosthodontic results of a prospective study,'' J. Am. Dent. Assoc., **129**, pp. 1097–1102.
[16] O'Callaghan, J., Goddard, T., Birichi, R., Jagodnik, J. J., and Westbrook, S., 2002, ''Abutment hammering tool for dental implants,'' *American Society of Mechanical Engineers, IMECE-2002 Proceedings Vol. 2, Nov. 11–16, 2002*, Paper No. DE-25112.
[17] Bozkaya, D., and Müftü, S., 2003, ''Mechanics of the tapered interference fit in dental implants,'' J. Biomech., **36**(11), pp. 1649–1658.
[18] Shigley, J. E. and Mischke, C. R., 2001, *Mechanical Engineering Design*, McGraw-Hill, Boston, MA.
[19] Gamer, U., and Müftü, S., 1990, ''On the elastic-plastic shrink fit with supercritical interference,'' ZAMM, **70**(11), pp. 501–507.
[20] Rabinowicz, E., 1995, *Friction and Wear of Materials*, John Wiley and Sons, NY.
[21] Adams, G. G., Müftü, S., and Mohd Azar, N., 2003, ''A Scale-Dependent Model for Multi-Asperity Model for Contact and Friction,'' J. Tribol., **125**, pp. 700–708.
[22] Pennock, A. T., Schmidt, A. H., and Bourgeault, C. A., 2002, ''Morse-type tapers: Factors that may influence taper strength during total hip arthroplasty,'' J. Arthroplasty, **17**, pp. 773–778.